IJE TRANSACTIONS B: Applications Vol. 32, No. 2, (February 2019) 286-295

International Journal of Engineering

Journal Homepage: www.ije.ir

Performance Analysis of a Novel Three-phase Axial Flux Switching Permanent Magnet Generator with Overlapping Concentrated Winding

H. Fekri[a], M. A. Shamsi-Nejad[*a], S. M. Hasheminejad[b]

[a] *Department of Electrical and Computer Engineering, University of Birjand, Birjand, Iran*
[b] *Department of Energy, Material and Energy Research Center, Karaj, Iran*

PAPER INFO

Paper history:
Received 11 October 2018
Received in revised form 15 November 2018
Accepted 03 January 2019

Keywords:
Wind Energy
Permanent Magnet Generator
Flux Switching
Design of Experiments
Response Surface Method

ABSTRACT

This paper proposes a novel axial flux switching permanent magnet generator for small wind turbine applications. Surface mounted axial flux switching permanent magnet (SMAFSPM) machine is a new type of these machines that is introduced in this paper. One of the most important challenges in optimal designing of this kind of machines, is ease of construction and maintenance. One of the main features of this machine is putting the magnets on the surface, which makes the construction of the machine easier. The overlapped three-phase winding improves the quality of voltages and power of the machine.To reach the optimum dimensions of machine, centeral composite design (CCD) and response surface methodology (RSM) combined with 3D finite element methods have been used.

***doi**: 10.5829/ije.2019.32.02b.14*

1. INTRODUCTION

With an increase of environmental sensitivities, societies are requesting stable solutions to the long term problems of the fossil fuels. One of the main branches of study has been research about new advanced machines, which reduce pollutions with respect to traditional machines. Generators which produce more efficient renewable energies in the source side and effective permanent magnet machine in advanced electrical vehicles [1] in the consumption side are sharing a common solution. The new electrical generator or machine with simple but up-to-date high capability is a prominent need. Over the last 10 years, several axial flux machine topologies including permanent magnet synchronous motor and generator [2-6], overlapped and non-overlapped concentrated [7-10], and variable flux machines [11-13] have made significant advances in this subject of research.

*Corresponding Author Email: mshamsi@birjand.ac.ir (M. A. Shamsi-Nejad)

Axial flux switching permanent magnet machine (AFSPM) is one of the permanent magnet (PM) machine types that introduced and developed in recent years [14, 15] for various applications from low speed wind turbine direct drive conversion [16], medium speed automotive traction, alternator and electric vehicle [17] to high speed like aircraft starter-generator[۱۸] some special topologies like dual rotor [19, 20] dual stator [21] fault tolerant [22] hybrid excited [23-25] and single phase PM motors [26] were proposed and tested. The optimized designs reduced cogging torque [27-30] by innovative and heuristic technics.

One of the problems in construction of AFSPM machines is the inserted PM in the middle of stator yoke that restricts the magnet dimensions. The present research continues previous works [31, 32] (Figure 1) for an optimal design of axial flux switching machines and introduces a new topology which reduces the difficulty of fabrication and produces smother three-phase voltage and power output. A new overlapping winding introduced that not only has minimum disturbing effect on the machine efficiency but also

Please cite this article as: H. Fekri, M. A. Shamsi-Nejad, S. M. Hasheminejad, Performance analysis of a novel three-phase axial flux switching permanent magnet generator with overlapping concentrated winding, International Journal of Engineering (IJE), IJE TRANSACTIONS B: Applications Vol. 32, No. 2, (February 2019) 286-295

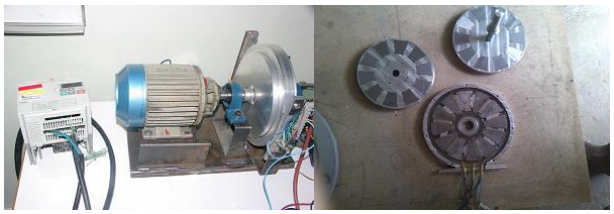

Figure 1. Previous work on AFSPM machines [29,30]

decreases high order harmonic effects and total harmonic distortion (THD) of the back-electromotive force (EMF). So the advantages of proposed machine can describe briefly as: 1) economic design and construction with respect to the other simillar designs, 2) lighter rotor than the other axial flux permanent magnet machines 3) capability of increasing of power at the same radius and rotor (by increasing the magnet thickness) and the disadvantage is increasing in temperature of magnets in vicinity of windings and lower power that can be solve this problem with heat removal techniques.

Response surface methodology (RSM) is a collection of mathematical and statistical techniques useful for the modeling and analysis of problems in which a response of interest is influenced by several variables and the objective is to optimize this response. RSM has been used for experimental science like biology, chemistry, materials, metallurgy, medical etc; but recent years has been taken into considered as a method for other fields like mechanical [33] and electrical engineering. [34, 35]

This paper is organized as follows: Section II presents topology of proposed machine and principle of operation. Section III provides main formulation of electromagnetic design and the influence of parameters on machine performance, the final dimension and simulation of the proposed machine using finite element analysis. The conclusion follows in section IV.

2. TOPOLOGY AND PRINCIPLES

2. 1. Topology The topology of proposed surface mounted AFSPM machine is made up of single stator and single rotor. Main difference between this structure and other AFSPM machines is the stator which is composed of a simple yoke and permanent magnets are placed on its surface. The magnetic flux direction of PMs is aligned with the axis and adjacent PMs have contrary magnetization polarity. Concentrated windings are wound around two adjacent magnets. This simple structure makes it easy to construct and decrease the price of production than other existing structures of AFSPMs. The rotor has the same structure as the other flux switching permanent magnet machines. Like the other AFSPM machines there are neither magnets nor windings in the rotor. Figure 2 shows a view of three phase 12/10 stator/rotor poles of surface mounted AFSPM.

2. 2. Operation Principle SMAAFSPM machines principle of operation is described in three situations as illustrated in Figure 3. It can be shown, the flux linkage varies from positive maximum (Figure 3a) to zero (Figure 3b) and negative maximum (Figure 3c). If the rotor tooth be in the situation (a) flux linkage comes from top of the winding to bottom. In the situation (b) because of the flux path is in the middle of winding, there are no flux linkage and in the situation (c) the flux linkage is maximum from bottom to top of the winding i.e. in the negative direction. So it offers bipolar flux linkage, which is similar to the conventional FSPM machines. The situation (b) is not a constructive position. Because we have a cycle path and no winding to link with it, that decreases performance of machine, so for better efficiency we can use overlap windings (Figure 4) A complete winding diagram of a 3 phase and 12 stator pole is shown in Figure 5.

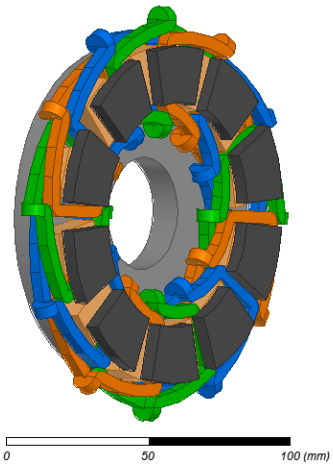

Figure 2. 3D view of novel AFSPM machine

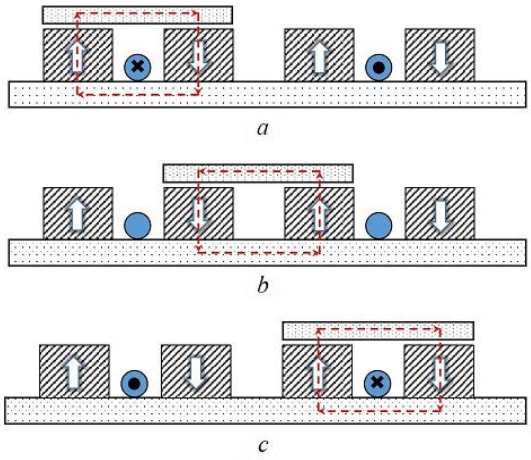

Figure 3. Principle operation of AFSPM machine

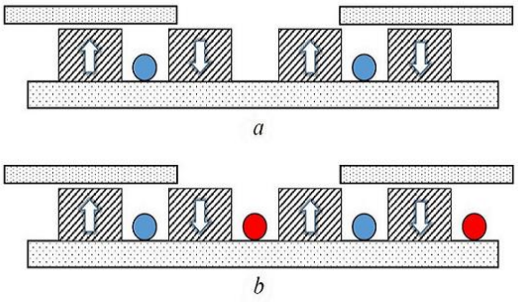

Figure 4. Winding diagram of proposed machine

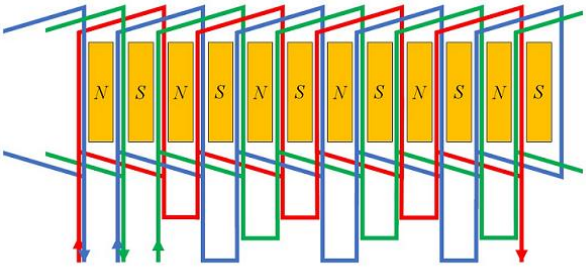

Figure 5. Winding diagram of proposed machine

3. DESIGN AND PERFORMANCE

3. 1. Electromagnetic Design and Optimization

Like the other kinds of axial flux permanent magnet machines, the main dimension of proposed design extracted from power equation. The outer diameter of machine is expressed as follows:

$$D = \sqrt[3]{\frac{240 P_2 N_s}{\sqrt{2}\pi^3 N_r k_d k_F k_{io}(1-k_{io}^{\ 2}) A_s B_{g\max} \alpha_i n \eta}} \quad (1)$$

where P_2 is the output power, N_s and N_r are respectively the number of stator and rotor poles, k_d is the leakage coefficient, k_F is the air gap flux density distribution coefficient, k_{io} the ratio of the inner and outer diameter, A_s maximum current density, B_{gmax} maximum air-gap flux density, α_i the area ratio of stator tooth and stator tooth-slot, n the speed of the rotor and η efficiency. The number of stators and rotor poles in flux switching machines denoted by the following formula:

$$N_s = N_r \pm k(k = 2,4,6,...) \quad (2)$$

and the rotor speed is given as follows:

$$n = \frac{60}{N_r} \quad (3)$$

where f is the electrical frequency of the electricity generated in the coils.

Base on Equations (1) and (3) and for each flux switching machine the stator outer diameter is:

$$D = \sqrt[3]{\frac{2\sqrt{2} P_2 N_s}{\pi^3 N_r k_d k_F k_{io}(1-k_{io}^{\ 2}) A_s B_{g\max} \alpha_i f \eta}} \quad (4)$$

Optimum size of rotor thickness, stator yoke and rotor split ratio obtained by considering several factors such as the effective produced flux and voltage, cogging torque reduction and harmonic content [36]. Figure 6 shows the influence of rotor thickness on the peak value of back-EMF and peak-peak of cogging torque when the other parameters are constant. When the rotor yoke thickness varies from 3mm to 10mm the reluctance becomes greater and therefore Back-EMF and linkage flux becomes weaker.

Cogging torque has different behavior, i.e. it increases with increase of in the rotor thickness. The reason can be discribe if we notice the peak value of cogging torque occurs when the maximum amount of magnetic flux enters the side of a rotor tooth. Varying the rotor thickness changes the magnitude of cogging torque by altering the distribution of the attractive force [37]. Figure 7 displays the effect of magnetic flux variations on cogging torque by changing in rotor thickness. Increasing the thickness of rotor, as displayed in Figure 7b, enlarges the area that the magnetic flux produces a greater attraction.

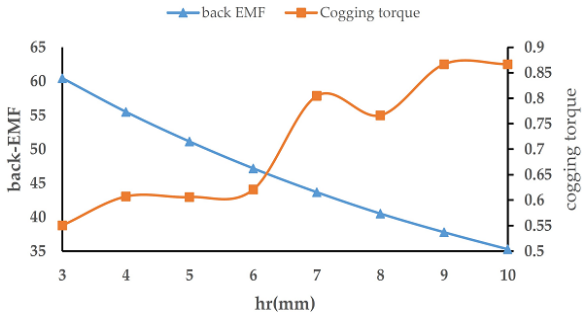

Figure 6. Influence of rotor thickness on cogging torque and back-EMF

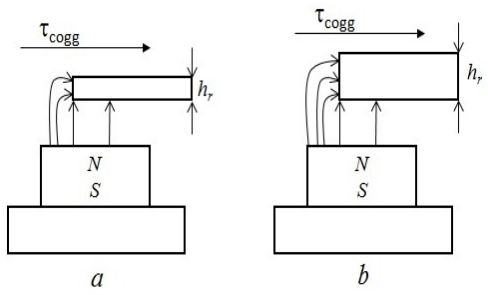

Figure 7. Variation of rotor thickness and its effects on cogging totque

Thus, in this way the magnitude of cogging torque increases. Lower thickness of rotor means lower mass and lower weight that reduces mechanical losses. Similar method is used for stator yoke and rotor split ratio. Figure 8 shows the effect of rotor tooth angle on cogging torque and back-EMF when varies from 10 to 30 mechanical degrees. Cogging torque has quite different behavior with variation of rotor tooth angle. The effect of stator yoke thickness when it varies from 5 to 20mm is shown in Figure 9.

RSM has been one of the best tools for finding the optimal variables in experimental researchs and design of electrical machines in recent years. Suppose the response, y is a function of some independent variables $x_1, x_2, \ldots, x_k$:

$$y = f(x_1, x_2, \ldots) + \varepsilon \quad (5)$$

where ε is the error in the response y. Often the function of f(x) represents by a polynomial, for example such as the second-order model:

$$f(x_1, x_2, \ldots) = \beta_0 + \sum_{i=1}^{k} \beta_i x_i + \sum_{i=1}^{k} \beta_{ii} x_i^2 + \sum\sum_{i<j} \beta_{ij} x_i x_j + \varepsilon \quad (6)$$

where β_0, β_i, β_{ii}, and β_{ij} are the regression coefficients e_i estimated, x_i and x_j are variables.

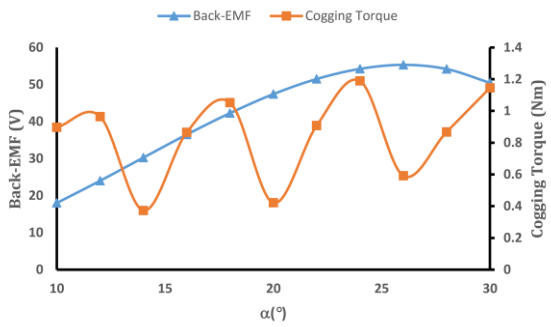

Figure 8. Variation of cogging torque and back-EMF with rotor tooth angle

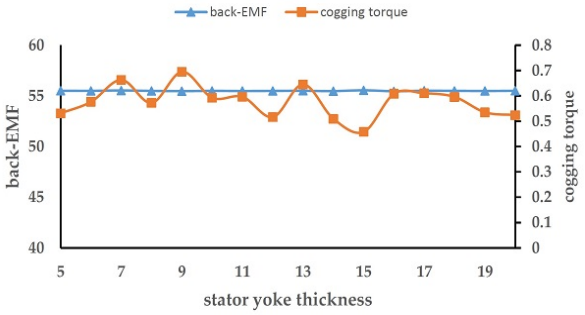

Figure 9. Effect of stator yoke thickness on the back-EMF and flux linkage

The regression coefficients are the relationship beetwen response and variables that obtain by experimental criteria. The central composite design (CCD) is the most popular class of designs used for fitting a second-order model. The philosophy of CCD is to determine the level of each variable and combination of them in each experiment.

After variable level selection the experiments completed by the 3D FEM analysis and finaly the coefficients are determined by the analysis of variance (ANOVA). Table 1 shows the variable level determination by CCD and the results for each combination of selected inputs.

Back-EMF: ANOVA table for back-EMF is shown in Table 2. Logaritmic tranasformation and quadratic model was selected for this analysis. The parameters with p-value, or calculated probability, less than 0.05 are significant and effective. It deduced from the results that the effective parameters are h_r ,α and h_{yok} has no significant effect on back-EMF.

The equation that extracts from RSM and relates the back-EMF to selected variables is written as follows:

$$\log(EMF) = 0.762922 - 0.125196 \times h_r + 0.114265 \times \alpha - 0.00403003 \times \alpha \times h_r - 0.00302918 \times \alpha^2 \quad (7)$$

TABLE 1. Result of CCD and experiments

h_r (mm)	h_{yoke} (mm)	α (°)	EMF (V)	$T_{coggP-P}$ (Nm)
11	11	20	27.8394	0.618294
5	16	29	50.2132	0.952591
11	11	20	27.8394	0.618294
5	5	11	20.1012	0.972083
11	11	20	27.8394	0.618294
20	11	20	12.3103	0.736134
11	11	20	27.8394	0.618294
5	16	11	20.0047	1.00003
16	5	11	1.55799	0.960902
11	11	20	27.8394	0.618294
11	20	20	27.8379	0.653461
11	11	20	27.8394	0.618294
1	11	20	23.884	0.854022
11	11	35	9.83402	0.656054
11	11	5	1.99318	0.800405
16	16	11	1.5172	0.920467
16	16	29	24.1645	0.952202
5	5	29	50.0077	1.11652
16	5	29	24.0892	1.04049
11	1	20	9.9774	0.414526

TABLE 2. ANOVA for Reduced Cubic model of back-EMF

Source	Sum of Squares	df	Mean Square	F-value	p-value
Model	3.41	4	0.8527	21.80	< 0.0001
A-hr	0.6867	1	0.6867	17.55	0.0008
C-alpha	0.5641	1	0.5641	14.42	0.0018
AC	0.3184	1	0.3184	8.14	0.0121
C^2	0.8835	1	0.8835	22.58	0.0003
Residual	0.5868	15	0.0391		
Lack of Fit	0.5868	10	0.0587		
Pure Error	0.0000	5	0.0000		
Cor Total	4.00	19			

Figure 10 shows 3D and contour plot of the back-EMF response vs design factors obtained from the above formula. It's clear that the back-EMF improves by increasing rotor tooth angle (α) and decresing rotor thickness (h_r).

Cogging Torque: The same approach is adopted for cogging torque and the results are shown in Table 3 and Figure 11, respectively. Quadratic model without any transformation has been selected for best resolution.
The response of cogging torque denoted as follows:

$$CoggingTorque = 1.62647 - 0.0898353 \times h_r - 0.0490523 \times \alpha + 0.0040462 \times h_r^{\,2} + 0.0012193 \times \alpha^2 \quad (8)$$

Figure 12 shows the effect of all factors on responses. As can be seen the factor of h_{yok} has no effect on back-EMF and cogging torque. h_r has the negetive effect on back-EMF. But α has positive effect on back-EMF from begin to about 22 degrees and negative effect in continue. The effect of h_r and α on cogging torque is negetive in the first half of interval and becomes positive in the other but the variations is very small. The effects of factors on cogging torque is independent from each other.

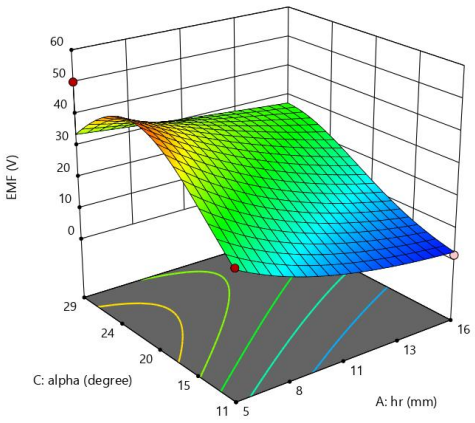

Figure 10. Response of Back-EMF against rotor tooth angle (α) and thickness (h_r)

TABLE 3. ANOVA for Reduced Cubic model of cogging torque

Source	Sum of Squares	df	Mean Square	F-value	p-value
Model	0.3408	4	0.0852	3.49	0.0332
A-hr	0.2271	1	0.2271	9.30	0.0081
C-alpha	0.1363	1	0.1363	5.58	0.0321
A^2	0.2180	1	0.2180	8.93	0.0092
C^2	0.1420	1	0.1420	5.82	0.0292
Residual	0.3662	15	0.0244		
Lack of Fit	0.3662	10	0.0366		
Pure Error	0.0000	5	0.0000		
Cor Total	0.7070	19			

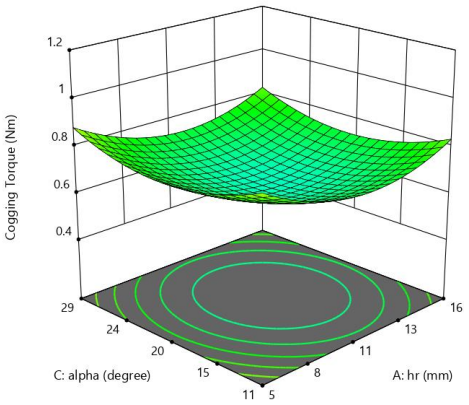

Figure 11. Response of cogging torque against rotor tooth angle (α) and thickness of stator yok(h_r)

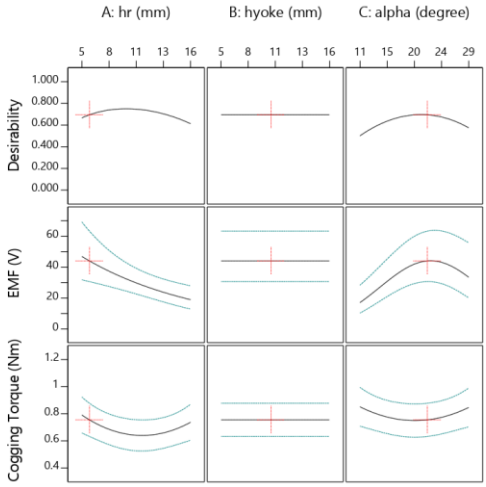

Figure 12. The effects of factors on responses

Finally optimum dimention illustrated in Table 4 base on RSM method.

3. 2. Static performance and comparison For better investigation of the proposed machine performance based on 3-D FE analysis, electromagnetic performance of the machine was evaluated. To conduct a comprehensive comparison for different design of overlapping winding (OW) and non-overlapping winding (NOW) two separate analyses of machines with the same dimension and excitation have been done. Total number of turns for each phase was kept the same. The key design parameters of these proposed machine based on optimization are illustrated in Table 5 and a 3-D finite element model of the machine for this analysis is illustrated in Figure 13 and Flux density distribution of the propose topology at each position is shown in Figure14.

TABLE 4. optimum facors

Factor	Value
h_r	9.5mm
h_{yok}	10.5mm
α	22.5°

TABLE 5. Specification and design parameter of machines

Parameter	Value	df	Mean Square	F-value	p-value
Outer diameter	140 mm	4	0.0852	3.49	0.0332
Inner diameter	70 mm	1	0.2271	9.30	0.0081
Air gap length	1 mm	1	0.1363	5.58	0.0321
Stator length	10 mm	1	0.2180	8.93	0.0092
Rotor length	10 mm	1	0.1420	5.82	0.0292
Magnet dimension	30×10×10 mm	15	0.0244		
Stator winding turns	OW: 800 turn per pole NOW: 1600 turn per pole	10	0.0366		
Stator pole arc	30°	5	0.0000		
Stator pole number	12	19			
Rotor pole number	10				
Rotor pole arc	22°				
Rated speed	300 rpm				
Rated voltage	50 V				

For a phase winding when rotor pole aligned with two magnets that situated in one side of winding, magnetic linkage flux is at maximum value. It decreases until The axis of rotor pole exactly reach to the center of winding. In this situation there is no flux linkage as shown in Figure 14b. In Figure 14c when the rotor pole is aligned with the magnets on the other side, flux linkage is maximum. Flux density distribution on the rotor and the stator cores are shown in Figure 15 at no-load condition. The maximum flux density located in the rotor and stator tooth did not exceed 2T. Overlapping design not only decreases THD of flux linkage and back-EMF but also inductances in the same losses and radius.

Figures 16 and 17 show the flux linkage and back-EMF of two design and Figure 18 compares the harmonic content of back-EMF.

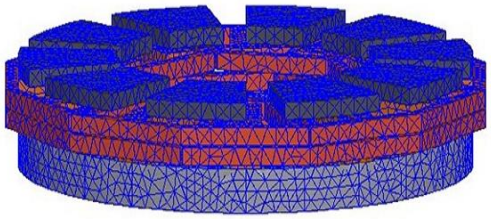

Figure 13. 3D finite element model of SMAFSPM

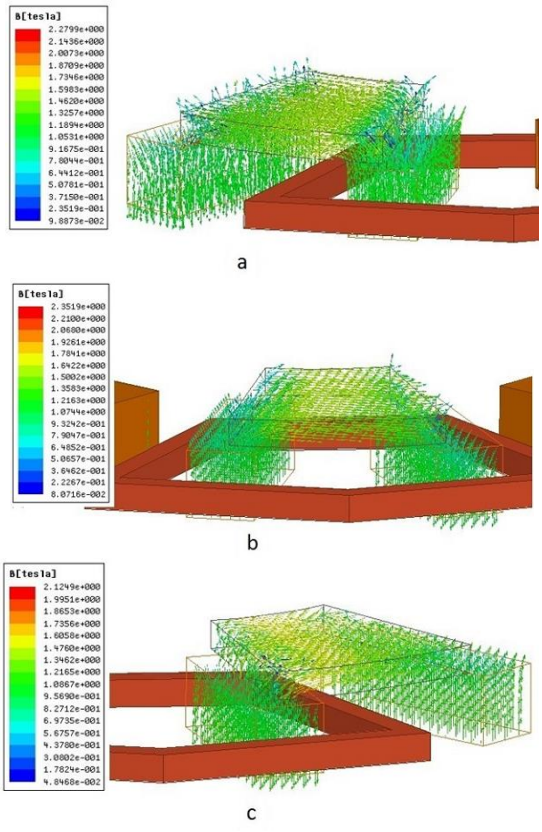

Figure 14. Flux linkage distribution in different situation

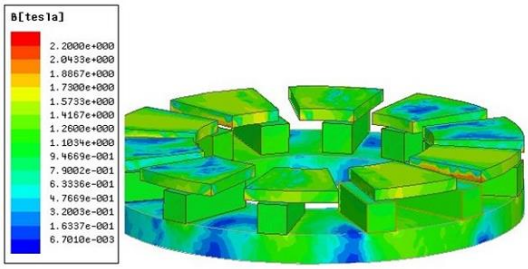

Figure 15. Flux density distribution

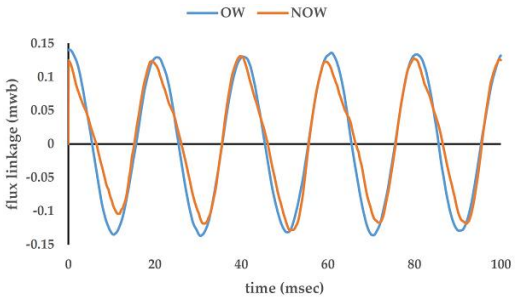

Figure 16. Flux density distribution of two designs

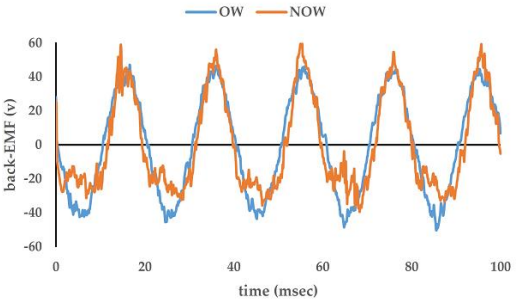

Figure 17. Back-EMF comparison of two designs

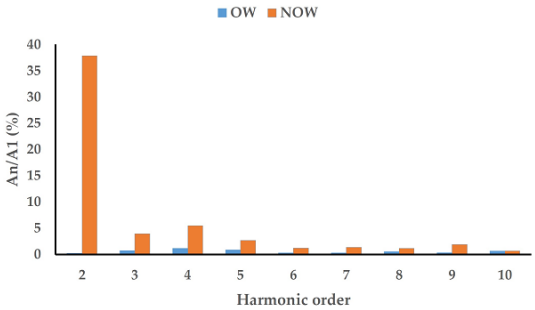

Figure 18. Harmonic content of back-EMF

The results show that wave form of overlapping winding is more sinusoidal and the harmonic content is better than the other design. The reason can be described as follows: phase voltage is sum of coils voltage as shown in Figure 19 and harmonic content of each coil voltage is shown in Figure 20; but closer look at real and imaginary component of harmonic contents. Figure 21 shows that the second order harmonic of each coil eliminates by the other, so the overall second order harmonic of OW is almost equal to zero.

The effects of the OW design on cogging torque are investigated as well in Figure 22. The cogging torque of NOW machine is a little greater than the OW design but this small difference is negligible, as the main structure of machine that makes the cogging torque is the same.

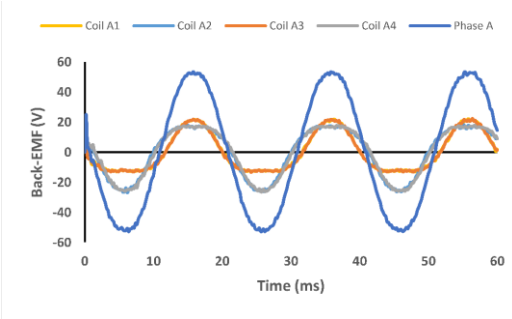

Figure 19. Back-EMF of phase A and coils

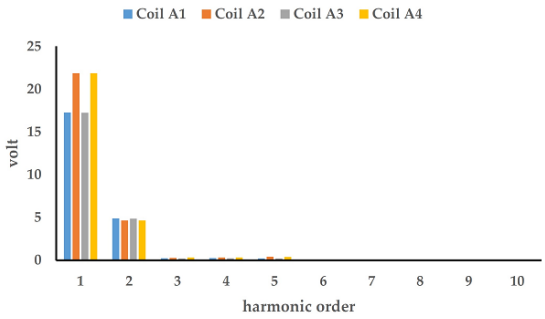

Figure 20. Harmonic content of each coils

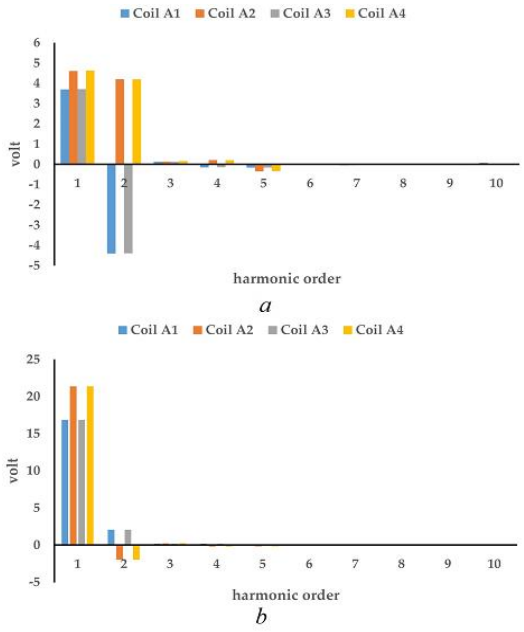

Figure 21. a) real and b)imaginary part of harmonic content of each coils

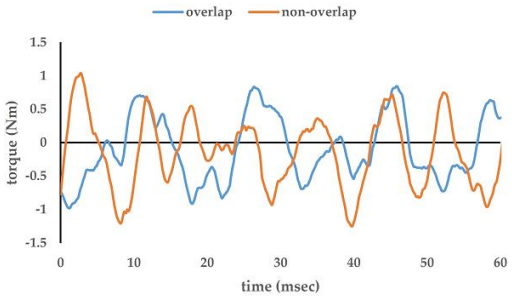

Figure 22. Cogging torque comparison

Figure 23 compares per turn self and mutual inductances of the designs and Figure 24 compares overall inductances. Although per turn self-inductance of NOW is smaller than OW's and mutual inductance is the same but the results for overall inductances show inverse effect i.e the absolute value of overall NOW inductances are twice of OW's. This is proven as we knew that the self-inductance is proportional to the square of winding turns and mutual inductance is proportional to multiple of two windings turns. So in the similar situation the winding turns in OW is half of turns in NOW design. Therefore, the results in OW is quarter of NOW and the winding turns in OW is twice of NOWdesign so one estimates that the inductances in OW is twice of NOW; for example, if the winding turns of OW be N then the turns of NOW will be 2N; therefor, OW inductance is proportion to N^2+N^2 or $2N^2$ that is half of NOWinductance which is proportion to $(N+N)^2$ or $4N^2$.

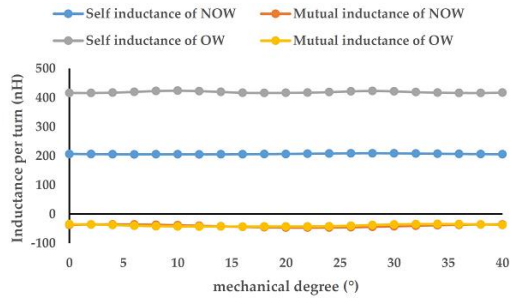

Figure 23. Per turn self and mutual inductances

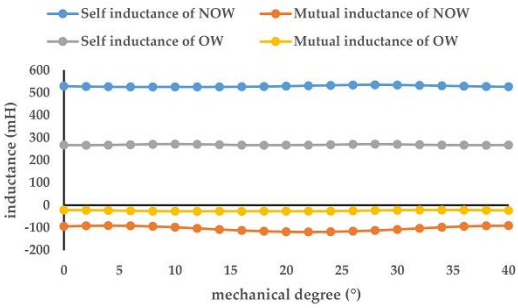

Figure 24. Overall self and mutual inductances

The end effect is not an important problem in this structure and for this two designs is exactly equal. OW design for SMAFPM structure doesn't have the effect of other OW topologies [38]. d-axis and q-axis inductances are shown in Figure 25.

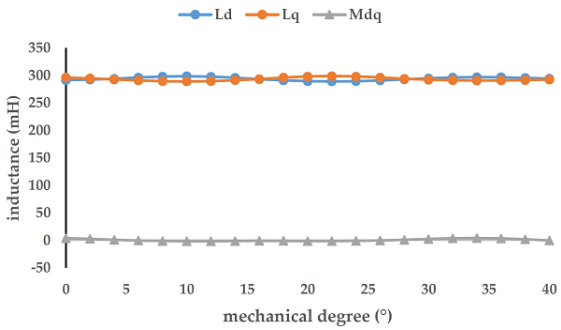

Figure 25. d and q axis inductances

4. CONCLUSION

In this paper a new structure of axial flux switching permanent magnet machine was introduced. The main feature of this structure is the location of magnets that are placed on the stator surface. in previous version of AFSPM machines the excitation located between stator segments which it made the construction of machine difficult. For a proper estimation of the machine specifications and finding optimum size of new machine a RSM combined with 3D FEM analysis have been done. OW and NOW design have been performed and compared. The results showed the OW design of this structure is more efficient and suitable than the other. THD of OW is 1.9 % in comparison with 38.6% of NOW, and inductances are 50% smaller than the other design. OW makes the machine smaller than NOW. The novelty of this work is its design that makes it less complex and its product inexpensive thus more economic than the other designs. It is suitable for soft magnetic composite (SMC) materials usage that needs compression or machinary in manufacturing. The other benefit of this design is the surface magnets that makes it possible to change the magnet thickness for a different power easily. This work is a preliminary design for construction of a prototype.

5. REFERENCES

1. Patel, A.N. and Suthar, B.N., "Design optimization of axial flux surface mounted permanent magnet brushless dc motor for electrical vehicle based on genetic algorithm", ***International Journal of Engineering***, ***Transactions A: Basics***, Vol. 31, No. 7, (2018), 1050-1056.
2. Kahourzade, S., Mahmoudi, A., Ping, H.W. and Uddin, M.N., "A comprehensive review of axial-flux permanent-magnet

machines", ***Canadian Journal of Electrical Computer Engineering***, Vol. 37, No. 1, (2014), 19-33.

3. Daghigh, A., Javadi, H. and Torkaman, H., "Design optimization of direct-coupled ironless axial flux permanent magnet synchronous wind generator with low cost and high annual energy yield", ***IEEE Transactions on Magnetics***, Vol. 52, No. 9, (2016), 1-11.
4. Zhu, Z. and Howe, D., "Electrical machines and drives for electric, hybrid, and fuel cell vehicles", ***Proceedings of the IEEE***, Vol. 95, No. 4, (2007), 746-765.
5. Kim, J.S., Lee, J.H., Song, J.-Y., Kim, D.-W., Kim, Y.-J. and Jung, S.-Y., "Characteristics analysis method of axial flux permanent magnet motor based on 2-d finite element analysis", ***IEEE Transactions on Magnetics***, Vol. 53, No. 6, (2017), 1-4.
6. Kouhshahi, M.B., Bird, J.Z., Acharya, V., Li, K., Calvin, M. and Williams, W., "An axial flux-focusing magnetically geared motor", in Energy Conversion Congress and Exposition (ECCE), IEEE, 307-313 ., (2017)
7. Xia, B., Shen, J.-X., Luk, P.C.-K. and Fei, W., "Comparative study of air-cored axial-flux permanent-magnet machines with different stator winding configurations", ***IEEE Transactions on Industrial Electronics***, Vol. 62, No. 2, (2015), 846-856.
8. Shao, L., Hua, W., Zhu, Z., Zhu, X., Cheng, M. and Wu, Z., "A novel flux-switching permanent magnet machine with overlapping windings", ***IEEE Transactions on Energy Conversion***, Vol. 32, No. 1, (2017), 172-183.
9. Kim, J.H., Choi, W. and Sarlioglu, B., "Closed-form solution for axial flux permanent-magnet machines with a traction application study", ***IEEE Transactions on Industry Applications***, Vol. 52, No. 2, (2016), 1775-1784.
10. Parviainen, A., Pyrhonen, J. and Kontkanen, P., "Axial flux permanent magnet generator with concentrated winding for small wind power applications", in Electric Machines and Drives, 2005 IEEE International Conference on,1191-1187, (2005)
11. Liu, X., Wang, M., Chen, D. and Xie, Q., "A variable flux axial field permanent magnet synchronous machine with a novel mechanical device", ***IEEE Transactions on Magnetics***, Vol. 51, No. 11, (2015), 1-4.
12. Taran, N. and Ardebili, M., "A novel approach for efficiency and power density optimization of an axial flux permanent magnet generator through genetic algorithm and finite element analysis", in Industrial Electronics (ISIE), 2014 IEEE 23rd International Symposium on, 709-714, (2014)
13. Saifee, A.H., Mittal, A., Laxminarayan, S.S. and Singh, M., "Design of a novel field controlled constant voltage axial flux permanent magnet generator for enhanced wind power extraction", ***IET Renewable Power Generation***, Vol. 11, No. 7, (2017), 1018-1025.
14. Hao, L., Lin, M., Xu, D., Fu, X. and Zhang, W., "Static characteristics of a novel axial field flux-switching permanent magnet motor with three stator structures", ***IEEE Transactions on Magnetics***, Vol. 50, (2014), 1-4.
15. Zhang, W., Liang, X. and Lin, M., "Analysis and comparison of axial field flux-switching permanent magnet machine with three different stator cores", ***IEEE Transactions on Applied Superconductivity***, Vol. 26, No. 7, (2016), 1-6.
16. Lin, M., Hao, L., Li, X., Zhao, X. and Zhu, Z., "A novel axial field flux-switching permanent magnet wind power generator", ***IEEE Transactions on Magnetics***, Vol. 47, No. 10, (2011), 4457-4460.
17. Kim, J.H., Li, Y. and Sarlioglu, B., "Novel six-slot four-pole axial flux-switching permanent magnet machine for electric vehicle", ***IEEE Transactions on Transportation Electrification***, Vol. 3, No. 1, (2017), 108-117.
18. Fernando, N., Vakil, G., Arumugam, P., Amankwah, E., Gerada, C. and Bozhko, S.J.I.T.o.I.E., "Impact of soft magnetic material on design of high-speed permanent-magnet machines", ***IEEE Transactions on Industrial Electronics***, Vol. 64, No. 3, (2017), 2415-2423.
19. Hao, L., Lin, M., Li, W., Luo, H., Fu, X. and Jin, P., "Novel dual-rotor axial field flux-switching permanent magnet machine", ***IEEE Transactions on Magnetics*** ,Vol. 48, No. 11, (2012), 4232-4235.
20. Zhao, W., Lipo, T.A. and Kwon, B., "A novel dual-rotor, axial field, fault-tolerant flux-switching permanent magnet machine with high-torque performance", ***IEEE Transactions on Magnetics***, Vol. 51, No. 11, (2015), 4-10.
21. Wang, Y., Chen, M., Ching, T. and Chau, K., "Design and analysis of a new hts axial-field flux-switching machine", ***IEEE Transactions on Applied Superconductivity***, Vol. 25, No. 3, (2015), 1-5.
22. Zhang, W., Lin, M., Xu, D., Fu, X. and Hao, L" ,.Novel fault-tolerant design of axial field flux-switching permanent magnet machine", ***IEEE Transactions on Applied Superconductivity***, Vol. 24, No. 3, (2014), 1-4.
23. Liu, X., Diao, Y., Zhang, C., Chen, D., Zuo, L. and Yi, L., "Design optimisation of an axial flux-switching hybrid excitation synchronous machine at no-load", ***IET Electric Power Applications***, Vol. 8, No. 9, (2014), 342-348.
24. Zhao, J., Lin, M. and Xu, D., "Minimum-copper-loss control of hybrid excited axial field flux-switching machine", ***IET Electric Power Applications***, Vol. 10, No. 2, (2016), 82-90.
25. Zhang, W., Liang, X., Lin, M., Hao, L. and Li, N., "Design and analysis of novel hybrid-excited axial field flux-switching permanent magnet machines", ***IEEE Transactions on Applied Superconductivity***, Vol. 26, No. 4, (2016), 1-5.
26. Syed, Q.A.S., Kurtović, H. and Hahn, I., "New single-phase flux switching axial flux permanent magnet motor", ***IEEE Transactions on Magnetics***, Vol. 53, No. 11, (2017), 1-5.
27. Hao, L., Lin, M., Xu, D. and Zhang, W., "Cogging torque reduction of axial field flux-switching permanent magnet machine by adding magnetic bridge in stator tooth", ***IEEE Transactions on Applied Superconductivity***, Vol. 24, No. 3, (2014), 1-5.
28. Hao, L., Lin, M., Xu, D., Li, N. and Zhang, W., "Cogging torque reduction of axial-field flux-switching permanent magnet machine by rotor tooth notching", ***IEEE Transactions on Magnetics***, Vol. 51, No. 11, (2015), 1-4.
29. Xu, D., Lin, M., Fu, X., Hao, L., Zhang, W. and Li, N., "Cogging torque reduction of a hybrid axial field flux-switching permanent-magnet machine with three methods", ***IEEE Transactions on Applied Superconductivity***, Vol. 26, No. 4, (2016), 1-5.
30. Hao, L., Lin, M., Xu, D., Li, N. and Zhang, W., "Analysis of cogging torque reduction techniques in axial-field flux-switching permanent-magnet machine", ***IEEE Transactions on Applied Superconductivity***, Vol. 26, No. 4, (2016), 1-5.
31. Fekri, H. and HashemiNejad, S.M., "No load performance of a novel synchronous permanent magnet generator with soft magnetic composite", ***International Journal of Emerging Technology and Advanced Engineering***, Vol. 5, No. 3, (2015), 24-29.
32. Nejad, S.M.H. and Fekri, H., "Switching permanent magnet generator for small wind turbine ", ***International Journal of Inventive Engineering and Sciences***, Vol. 2, No. 10, (2014), 5-8.
33. Kazemian, M.E., Ebrahimi-Nejad, S. and Jaafarian, M., "Experimental investigation of energy consumption and performance of reverse osmosis desalination using design of

experiments method", ***International Journal of Engineering, Transactions A: Basics***, Vol. 31, No. 1, (2018), 79-87.

34. Zhang, C., Chen, Z., Mei, Q. and Duan, J., "Application of particle swarm optimization combined with response surface methodology to transverse flux permanent magnet motor optimization", ***IEEE Transactions on Magnetics***, Vol. 53, No. 12, (2017), 1-7.
35. Beigi, H. and Cheshmeh, M., "Design, optimization and fem analysis of a surface-mounted permanent-magnet brushless dc motor", ***International Journal of Engineering, Transactions B: Applications*** Vol. 31, No. 2, (2018), 339-345.
36. Patel, A. and Suthar, B.J.I.J.O.E., "Design optimization of axial flux surface mounted permanent magnet brushless dc motor for electrical vehicle based on genetic algorithm", ***International Journal of Engineering, Transactions A: Basics,*** Vol. 31, No. 7, (2018), 1050-1056.
37. Studer, C., Keyhani, A., Sebastian, T. and Murthy, S., "Study of cogging torque in permanent magnet machines", in Industry Applications Conference, 1997. Thirty-Second IAS Annual Meeting, IAS'97., Conference Record of the 1997 IEEE, (1997), 42-49.
38. Wu, Z., Zhu, Z. and Zhan, H., "Comparative analysis of partitioned stator flux reversal pm machines having fractional-slot nonoverlapping and integer-slot overlapping windings", ***IEEE Transactions on Energy Conversion***, Vol. 31, No. 2, (2016), 776-788.

Performance Analysis of a Novel Three-phase Axial Flux Switching Permanent Magnet Generator with Overlapping Concentrated Winding

H. Fekri[a], M. A. Shamsi-Nejad[a], S. M. Hasheminejad[b]

[a] *Department of Electrical and Computer Engineering, University of Birjand, Birjand, Iran*
[b] *Department of Energy, Material and Energy Research Center, Karaj, Iran*

P A P E R I N F O

Paper history:
Received 11 October 2018
Received in revised form 15 November 2018
Accepted 03 January 2019

Keywords:
Wind Energy
Permanent Magnet Generator
Flux Switching
Design of Experiments
Response Surface Method

چکیده

در این مقاله یک ژنراتور مغناطیس دائم شار سوئیچینگ دیسکی برای کاربرد توربین های بادی پیشنهاد شده است. مزیت مدل پیشنهادی استفاده از آهنربای سطحی در ساختمان ماشین است که هزینه ساخت آن را نسبت به دیگر ماشین های شار سوئیچینگ دیسکی کاهش می دهد. همچنین برای بهبود عملکرد ماشین روش سیم پیچی هم پوشانی پیشنهاد گردیده است و تأثیر موارد پیشنهاد شده بر روی عملکرد ماشین از جمله سطح ولتاژ، هارمونیک ولتاژ و گشتاور دندانه با استفاده از تحلیل المان محدود سه بعدی تحقیق و بررسی گردیده. برای بهینه سازی با استفاده از طرح مرکب مرکزی (CCD) از روش های پاسخ سطح (RSM) ضمن بررسی عوامل مؤثر بر نیروی محرکه الکتریکی (EMF) و گشتاور دندانه، ابعاد ماشین بهینه سازی شده است.

***doi**: 10.5829/ije.2019.32.02b.14*